

Soil properties and site characterization through Rayleigh waves

V. Roma, PhD

Geodata S.P.A., Turin, Italy

ABSTRACT: Surface wave methods based on Rayleigh waves propagation represent a promising tool to determine shear wave velocity and damping ratio profiles at a site at very small deformations. After introducing the theoretical basis of the uncoupled and coupled procedures, the results obtained at a site with the two procedures are compared.

1 INTRODUCTION

For many engineering applications the level of deformations in the soil is small (Mancuso 1992, Lancellotta 1995), especially when dealing with normal functionality of the structures. Within the range of very small deformations ($\gamma_{\text{cyclic}}=5 \cdot 10^{-6} \div 5 \cdot 10^{-5}$ Vucetic 1994), the mechanical behavior of the ground can be properly modeled by means of viscoelasticity (Christensen R.M. 1971). Specifically the shear tangent modulus and damping ratio profiles at a site can be determined by means of Rayleigh waves propagation (Rix et al. 2001), by assuming a layered half-space with horizontal, mono-phase, homogeneous, isotropic layers. Rayleigh waves propagate on the free surface of a medium and during propagation they are subjected to dispersion and attenuation. In the general framework of viscoelasticity dispersion and attenuation phenomena are correlated (Lai 1998), so that shear modulus and damping ratio are coupled mechanical properties of the soil. Nevertheless at very small deformations uncoupling dispersion and attenuation phenomena may represent a good approximation of soil behavior.

In this work both the coupled and the uncoupled procedures have been applied to a real site, in order to evaluate the shear wave velocity and shear damping ratio profiles at very small deformations (Roma 2001). The results may give useful information about the reciprocal influence of the dispersion and attenuation phenomena for approaching practical cases of soil-structure dynamic interaction.

2 EXPERIMENTAL SET UP

2.1 Source and spatial configuration of receivers

The spatial configuration of receivers depends on the type of source and the frequency range of interest. If the site response at low frequency ($f < 5 \div 10$ Hz) is sought, then the receivers are located in one or more concentric circles, in order to detect the microtremors caused by ambient noise (Zywicki & Rix 1999, Tokimatsu 1995). Instead if the frequencies of interest are relatively high ($10 \text{ Hz} < f < 100 \text{ Hz}$), then an active point source (harmonic or impulsive) is used and the receivers are positioned along a direct line diverging from the point source (Foti 2000).

The method followed in this work consists of exciting the soil at a point on the free surface (see fig.1) by means of an electro-dynamic shaker, which generates a harmonic excitation (Hebeler 2001). Both geophones and accelerometers can be used as receivers to measure either particle velocity or particle accelerations in the vertical direction at the several stations. By measuring the wave field at several locations, the dispersion and the attenuation of Rayleigh waves are evaluated, which strictly depend on the geometric and mechanical properties of the site (Aki K. & Richards P.G. 1980). It should be observed that both Rayleigh and body (P and S) waves are generated by the point source (Achenbach, J.D. 1999), but in the far field (about $0.5\lambda \div 2\lambda$) Rayleigh waves give the main contribution to the wave field and body waves are negligible (Stokoe II & Santamarina 2000, Rix 1988). From the wave field measurements the experimental displacement transfer function $T_{\text{exp}}(r, \omega)$ of the site is calculated. If the particle accelerations are measured, then the experimental

displacement transfer function of the system is (Lai et al. 2002):

$$T_{\text{exp}}(r, \omega) = \frac{-M(r, \omega) \cdot C_2(\omega)}{\omega^2 \cdot C_1(\omega)} \quad (1)$$

where $M(r, \omega)$ is the ratio of the particle acceleration measured at the receiver to the input force measured at the source. $C_1(\omega)$ and $C_2(\omega)$ are the frequency-dependent calibration factors of the accelerometers used to detect the particle motion and the accelerometer placed on the shaker, respectively. The factor $C_2(\omega)$ also includes the mass of the armature.

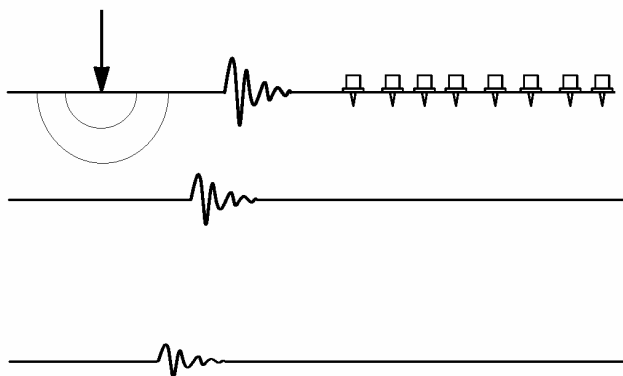


Figure 1. Scheme of the experiment in situ.

3 THEORETICAL BASIS OF THE METHOD

3.1 Dispersion and attenuation of Rayleigh waves

Dispersion phenomenon occurs when a wave train spreads out during propagation in space-time, because the several simple waves contained in the train travel at different phase and group velocities (Lighthill 1964, Brillouin & Sommerfeld 1960). The attenuation of mechanical waves is caused by geometric spreading (geometrical attenuation) and by dissipative forces among particles during their oscillations around the equilibrium position (material attenuation) (Goldstein 1950).

In a visco-elastic medium dispersion and material attenuation are inherently coupled, because the energy dissipation causes the phase velocity of Rayleigh waves to vary with the wavelength (Aki K. & Richards P.G. 1980). This kind of dispersion is called material dispersion to be distinguished from geometrical dispersion, which is due to the existence of wave-guides inside a layered half-space (Haskell, 1953, Thomson 1950, Tolstoy 1973). The geometric dispersion relation of Rayleigh waves, travelling on the free surface of a layered half-space, can be represented in terms of either frequency-wavenumber or frequency-phase velocity (Kausel and Roesset 1981). As a consequence of the dispersion phenomenon in a

layered half-space several Rayleigh modes of propagation may exist, so that the Rayleigh geometric dispersion relation is a multiple-branch function (Whitham 1974).

The material attenuation of Rayleigh waves is usually expressed in terms of a frequency dependent attenuation curve (see fig.4), which is made of the energy absorption coefficients calculated at different frequencies.

3.2 Coupled versus uncoupled procedure

Once the experimental transfer function of the site for travelling Rayleigh waves has been calculated either a coupled or an uncoupled procedure can be used to calculate the dispersion and attenuation curves and hence the shear wave velocity and damping ratio profiles at the site (Lai et al. 2002).

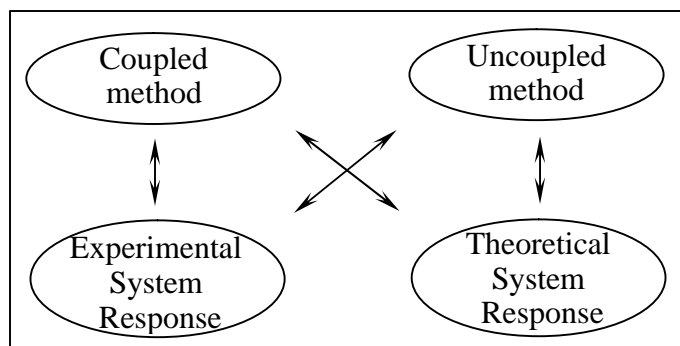


Figure 2. Graph of the possible combinations concerning method (coupled or uncoupled) and system response (experimental or theoretical).

The coupled method consists of minimizing the distance between the experimental displacement transfer function (1) and the theoretical evaluation of the same system response:

$$T_{\text{theo}}(r, \omega) = \frac{U_z(r, \omega, t)}{F_z \cdot e^{i\omega t}} = G(r, \omega) \cdot e^{-i \cdot \Psi(r, \omega)} \quad (2)$$

where ω is the circular frequency of excitation, F_z is the magnitude of the exciting force, $U_z(r, \omega, t)$ is the vertical displacement, $G(r, \omega)$ is the geometric spreading function of Rayleigh waves, $\Psi(r, \omega)$ is the apparent phase of the wave train, which contains all Rayleigh waves. It should be noted that near field effects due to P and S waves are not considered and only Rayleigh waves are taken into account in the theoretical formulation. Also the contribution of higher modes of Rayleigh is ignored in the apparent phase $\Psi(r, \omega)$, so that only the fundamental mode appears in the phase $\Psi(r, \omega) \cong k_R^*(\omega) \cdot r$ and (2) becomes:

$$T_{\text{theo}}(r, \omega) \cong G(r, \omega) \cdot e^{-i \cdot K_R^*(\omega) \cdot r} \quad (3)$$

Date: 3/4/2000
Test Site: Mud Island
Location: Memphis, TN
N - 35°09.388' W - 90°03.413'

Truck: GT Geostar
Test No: MudB1
GTRC No: E20-F47/F34

GWT: 8.0 m
Review: Paul Mayne
ASTM D 5778

Cone Type: Hogentogler 10T
Filter: Type 2
Supervisor: Paul Mayne
Operators: Alec McGillivray
Billy Camp

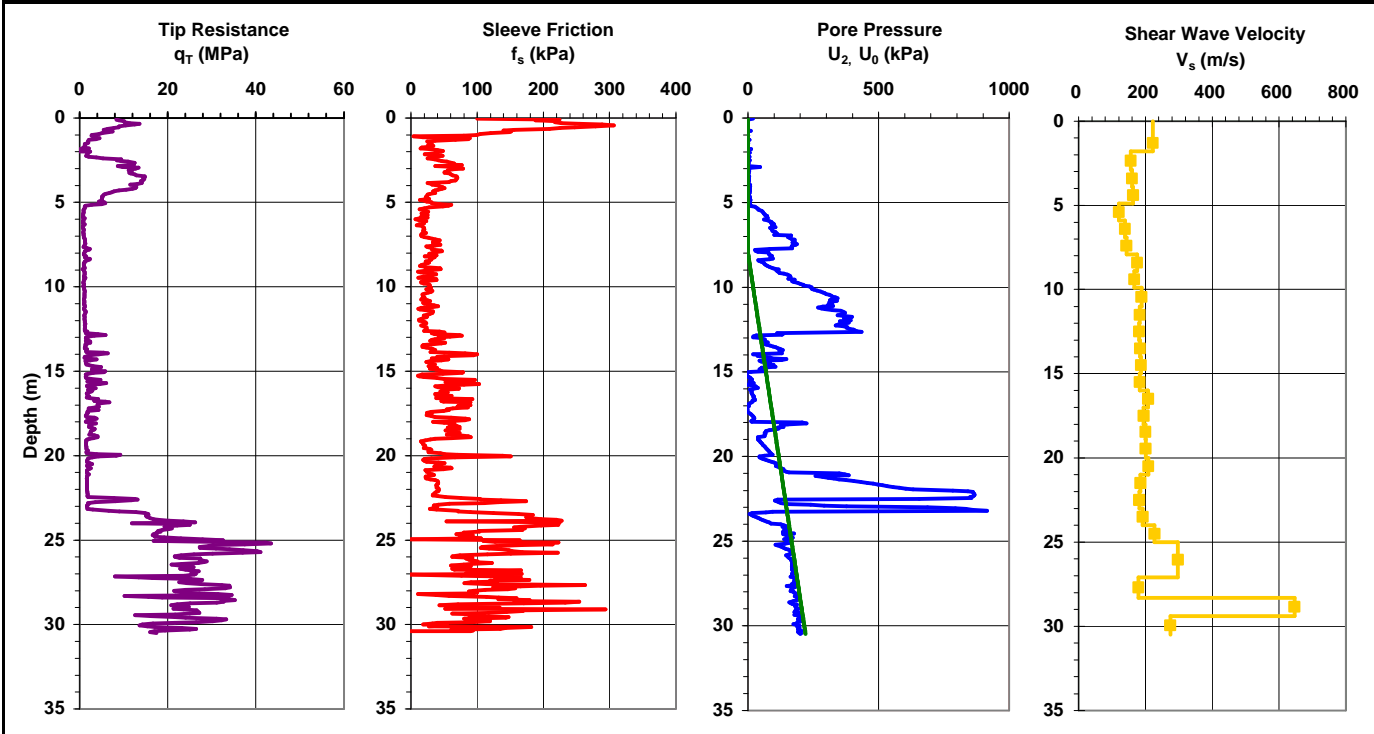


Figure 3. Results of SCPT tests performed at Mud Island site B (Mayne 2000).

The distance to be minimized is:

$$\sum_{i=1}^{i=N} |T_{\text{exp}}(r_i, \mathbf{w}) - T_{\text{theo}}(r_i, \mathbf{w})| = \text{distance}(\mathbf{w}) \quad (4)$$

in order to estimate the complex wavenumber:

$$K_R^*(\mathbf{w}) = \left[\frac{\mathbf{w}}{V_R(\mathbf{w})} - ia_R(\mathbf{w}) \right] \quad (5)$$

as a function of frequency. From the apparent complex wavenumber $k_R^*(\omega)$ the apparent dispersion and attenuation relations $V_R(\omega)$ and $\alpha_R(\omega)$ can be calculated (see fig.4). The term apparent indicates that in the geotechnical scale the distances over which the measurements are conducted are so limited that the wave train of simple waves has not yet completely dispersed. This means that it is not possible to distinguish among the several modes of Rayleigh waves, which still appear as a whole travelling disturbance (Roma 2001).

After evaluating the experimental dispersion and attenuation relations the subsequent coupled inversion procedure can be performed. The coupled inversion procedure is based on the Occam's optimization algorithm, which is a local search technique (Lai, 1998). The algorithm varies the shear wave velocity

and the shear damping ratio profiles of the site until an optimum misfit is reached between the experimental and the theoretical dispersion and attenuation curves, while the smoothness of the profiles is maximized. The non-linear optimization problem is solved by a linear expansion of the problem and the use of Lagrange's multiplier method (Lai 1998). The main difficulty of the coupled procedure is represented by the solution of the complex eigenvalue problem of Rayleigh waves, because the shear wave velocity and the damping ratio are considered as a unique variable, i.e. the complex shear wave velocity. The contribution of the several Rayleigh modes is not considered in the material attenuation and in the geometric spreading function $G(r,\omega)$ higher Rayleigh modes can be taken into account only by an iterative procedure, since the shear wave velocity profile is not known a priori at the beginning of the inversion procedure.

The uncoupled procedure assumes that in the range of very small deformations ($\gamma_{\text{cyclic}} = 5 \cdot 10^{-6} \div 5 \cdot 10^{-5}$) the coupling between dispersion and attenuation phenomena does not influence significantly the shear tangent modulus and the shear damping ratio profiles obtained at the end of the inversion procedure. The experimental apparent dispersion relation of Rayleigh waves at the site is calculated independently from the attenuation relation by a 2D Fourier transformation of the measured wave field from the time-space domain to the frequency-wavenumber domain (Roma et al. 2002). The theoretical apparent dispersion curve

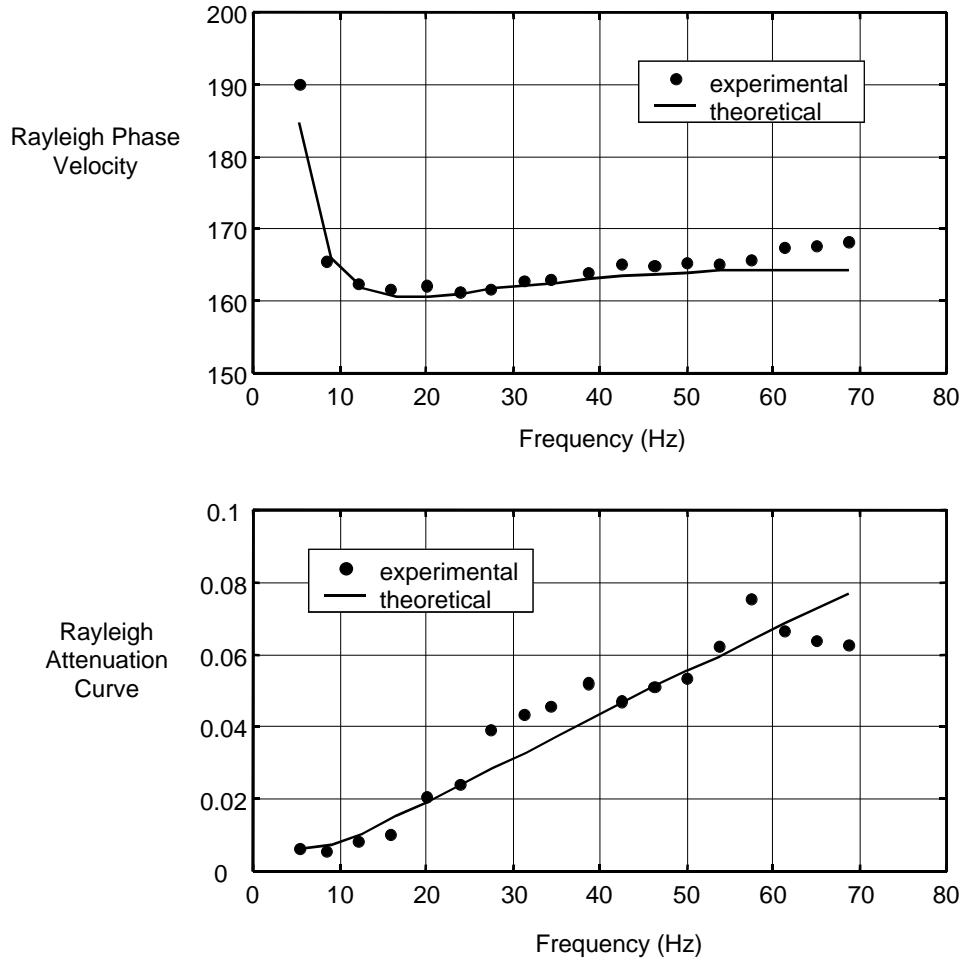


Figure 4. Experimental and theoretical dispersion (up) and attenuation (down) curves at Mud B site by means of the pure coupled method (Lai et al. 2002).

considers the effects of the higher modes of Rayleigh and can be determined by a 1D Fourier transformation from the frequency-space domain to the frequency wavenumber domain, applied to the theoretical displacement transfer function of the site (Roma et al. 2002). By means of an optimization algorithm the shear wave velocity profile of the site can be evaluated. In this paper a constrained least squares optimization algorithm is used, the Davidon-Fletcher-Powell (DFP) local search technique (Roma 2002). Once the shear wave velocity profile has been obtained (see table 1 and fig.5a in section 4), the experimental attenuation relation can be calculated, by minimizing the distance between the experimental and the theoretical displacement transfer functions of the site as described for the coupled procedure, but considering this time only the attenuation coefficient $\alpha_R(\omega)$ as the unknown in equation (5), since the phase velocity $V_R(\omega)$ has already been calculated in the first part of the uncoupled method. From the experimental attenuation curve $\alpha_R(\omega)$ the shear damping ratio profile is inverted by means of the same relationship used in the coupled procedure, with the diversity that in the uncoupled procedure the shear V_s and the compression V_p velocities are real quantities (Rix et al. 1999):

$$a(\omega) = \frac{w}{V_R^2} \left\{ \sum_i^N \left[V_{p,i} \cdot \left(\frac{\partial V_R}{\partial V_p} \right)_i \cdot \frac{D_{p,i}}{D_{s,i}} + V_{s,i} \cdot \left(\frac{\partial V_R}{\partial V_s} \right)_i \right] \cdot D_{s,i} \right\} \quad (6)$$

where i refers to the generic layer of the assumed layered half-space. The compression wave velocity profile V_p is estimated from the V_s profile via the knowledge of the Poisson' ratio ν ; the ratio between compression and shear damping ratios is assumed as $D_p / D_s = 1$ (Rix et al. 1999).

In principle the coupled and uncoupled procedures could be combined to give rise to mixed or hybrid procedures (see fig.2). In fact the coupled and uncoupled method refer both to the experimental evaluation of the dispersion and attenuation relations and to the inversion process for determining the shear wave velocity and damping ratio profiles. For example the coupled method can be adopted for the experimental part and the uncoupled procedure for the inversion process (see section 4) or vice versa the uncoupled method for the experimental step and the coupled procedure for the inversion part (Rix et al. 1999).

4 RESULTS AT A MUD ISLAND B SITE

In this section the results of the above explained uncoupled and coupled procedures will be reported with reference to Mud Island site B. The site is made of silt and sand and is located on an artificial island

on the Mississippi river near Memphis, TN, where a series of seismic cone penetration tests (SCPT) has been performed (Lai et al. 2002). The results from SCPT sounding are illustrated in figure 3 (Mayne 2000). The ground water table is located at a depth of 8m from the free surface.

The accelerometers measured the vertical particle motion generated by the electro-dynamic shaker in the range of frequency from 3.75Hz to 100Hz. The vector position in meters of the receivers set along a linear array respect to the source is:

$$x=[2.44, 3.05, 3.66, 4.57, 5.49, 6.71, 8.54, 10.37, 12.80, 15.24, 18.29, 21.34, 24.39, 28.96, 33.54].$$

The results of the pure coupled method applied at the same site have been obtained in a recent paper (Lai et al. 2002) and in figure 4 the experimental and theoretical dispersion and attenuation curves of Rayleigh waves are presented. The corresponding shear wave velocity and shear damping ratio profiles are reported in figure 5, together with the results of the SCPT tests.

The uncoupled procedure applied at the same experimental data has provided the experimental apparent dispersion curve plotted with the theoretical modes of Rayleigh (fig.7). It can be seen that the experimental curve coincides with the fundamental mode of Rayleigh waves, since the site is normally dispersive.

By means of a regression analysis applied to equation (6) the experimental attenuation coefficients have been evaluated at each frequency (fig.8) and the final uncoupled experimental attenuation curve is reported in figure 6 together with the coupled experimental attenuation curve of figure 3. It can be observed that the coupled attenuation curve comprises lower frequencies respect to the uncoupled attenuation curve, which means that in principle with the coupled method a deeper depth can be reached. Also both the experimental attenuation curves are characterized by an oscillating behavior as frequency increases and this is mainly due to the presence of higher modes of Rayleigh in the measured wave train. The theoretical attenuation curves are generally smoother than the experimental attenuation curves, since the theoretical model does not include the effects of higher modes of Rayleigh in evaluating the apparent phase $\psi(r,\omega)$, which has been simplified as $\psi(r,\omega) \cong k_R(\omega) \cdot r$. Nevertheless for normally dispersive sites or in any case at frequencies lower than the cut-off frequency of the second mode of Rayleigh the approximation gives the exact solution, for higher modes do not influence the apparent system response (Roma 2001). The uncoupled shear damping ratio has been evaluated by using the Occam's algorithm and the final profile is compared to the coupled profile in figure 5b.

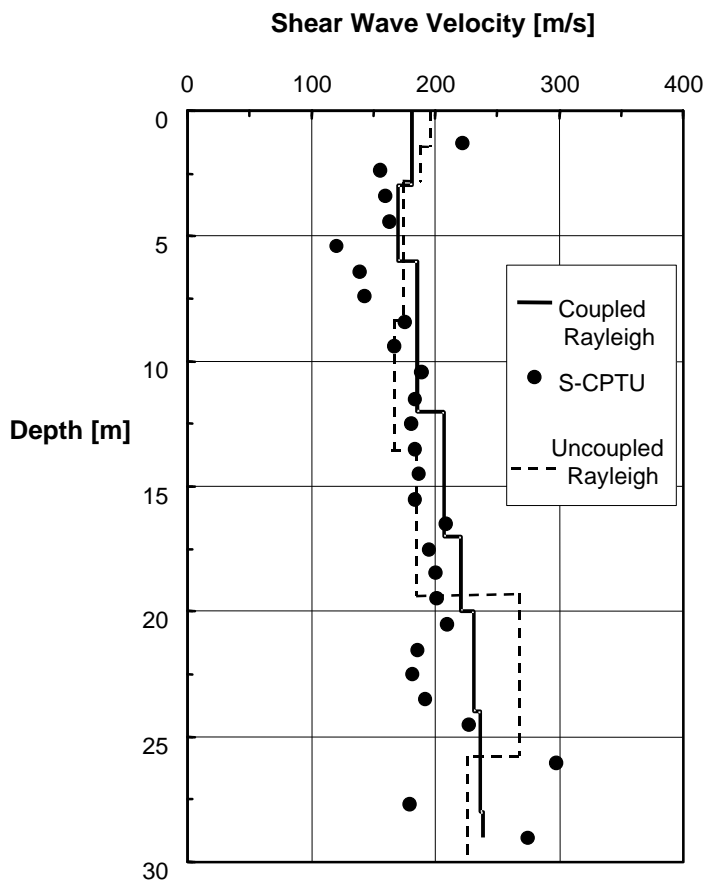


Figure 5a. Shear wave velocity profile at Mud B by SCPTU, Coupled Rayleigh waves and Uncoupled Rayleigh waves (modified from Lai et al. 2002).

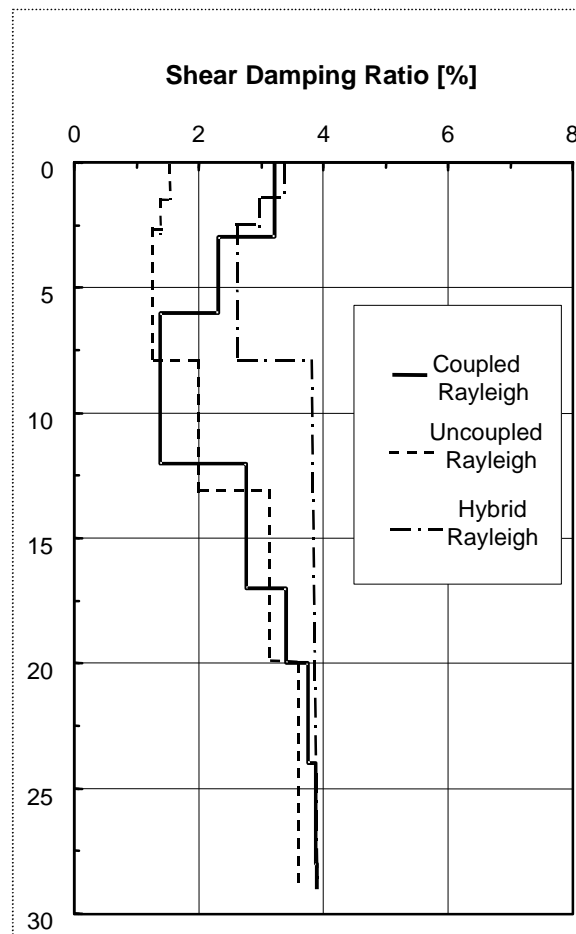


Figure 5b. Shear damping ratio profile at Mud B by Coupled Rayleigh waves, Uncoupled Rayleigh Waves and Hybrid Rayleigh waves (modified from Lai et al. 2002).

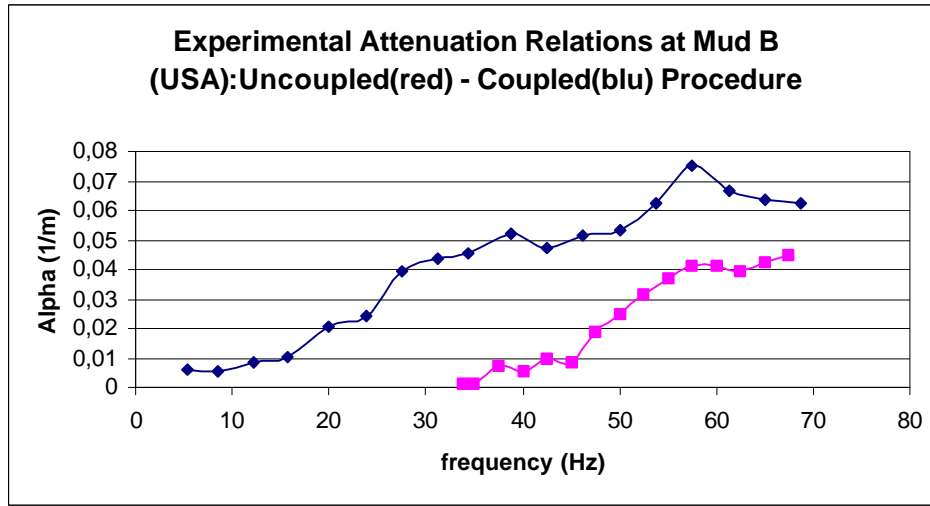


Figure 6. Experimental attenuation curves for Coupled method (upper curve) and uncoupled method (downer curve).

It is worthy to underline that experimental attenuation coefficients at frequencies higher than about 70Hz have been discarded from the analysis, because they generate high oscillations in the attenuation curve, that cannot be modeled by only the fundamental mode of Rayleigh. The frequencies above 70Hz contain information about the man-made upper ground of the site down to a depth of about $z=0.5\lambda=0.5 \cdot V_R/f=0.5 \cdot 170(\text{m/s})/70\text{Hz}=1.2\text{m}$.

Because the coupled experimental attenuation curve comprehends lower frequencies than the uncoupled experimental curve does, a hybrid approach has been followed for calculating the shear damping ratio profile. In fact the experimental attenuation curve has been calculated by means of the coupled procedure applied only to the measurements. Instead the inversion procedure has been performed by using the uncoupled method, once the shear wave velocity profile has been estimated independently. This approach offers the advantages of both the coupled procedure applied to the data and the uncoupled method, which allows for superposition of higher modes of Rayleigh to be taken into account to evaluate the geometric spreading function $G(r,\omega)$. Otherwise in the pure coupled technique the shear wave velocity profile is not known a priori and the effects of higher modes of Rayleigh cannot be considered in the geometrical dispersion by the simplified factor $1/\sqrt{r}$. The experimental and theoretical attenuation curves of the hybrid approach are plotted in figure 9 and the final shear damping ratio profile is illustrated in figure 5b with the pure coupled and pure uncoupled procedures (see also table 2).

From a comparison it can be realized that there are no appreciable differences among the pure uncoupled, the pure coupled and the hybrid methods. Hence it seems that at a small level of deformation (see equation (6)) the coupling effects between dispersion and attenuation phenomena are not sig-

nificant and the uncoupled procedure still remains a valid method for estimating the shear wave velocity and the damping ratio profiles.

The maximum shear strain during the experiment can be estimated on the ground surface from the measured maximum particle velocity $|v|_{\max}$ and the shear wave velocity V_{s1} of the surface layer:

$$\left|g_s\right|_{\max} = \frac{|v|_{\max}}{V_{s1}} = \frac{3.5 \cdot 10^{-3} \text{ m/s}}{(150 \div 200) \text{ m/s}} = (1 \div 5) \cdot 10^{-5} \quad (6)$$

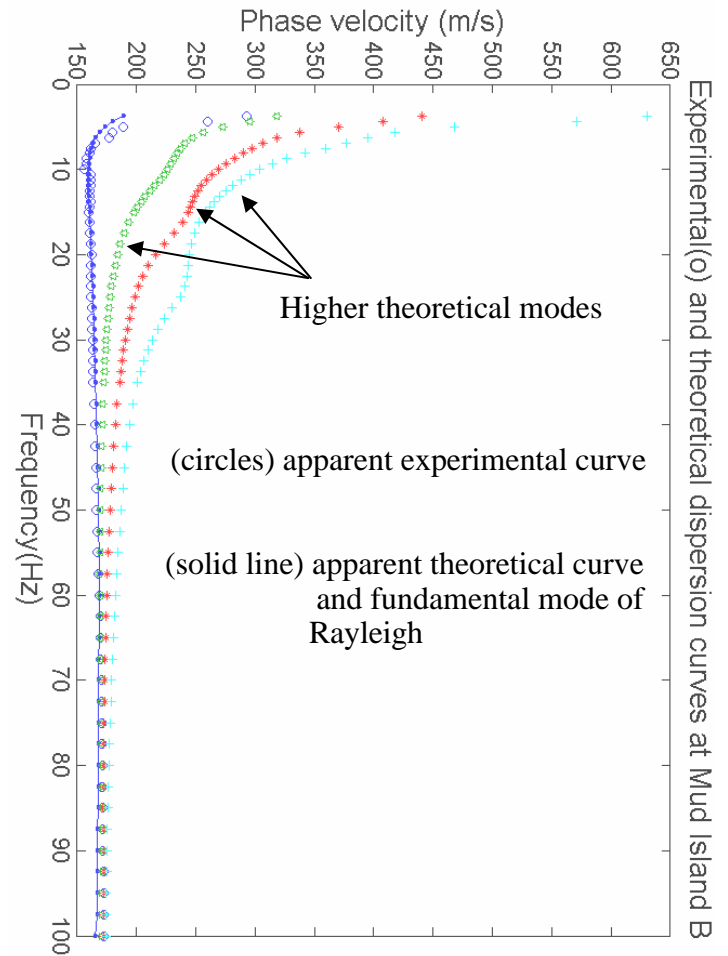


Figure 7. Uncoupled Rayleigh waves method: theoretical modes, experimental apparent dispersion curve (circles) and theoretical apparent dispersion curve (solid line).

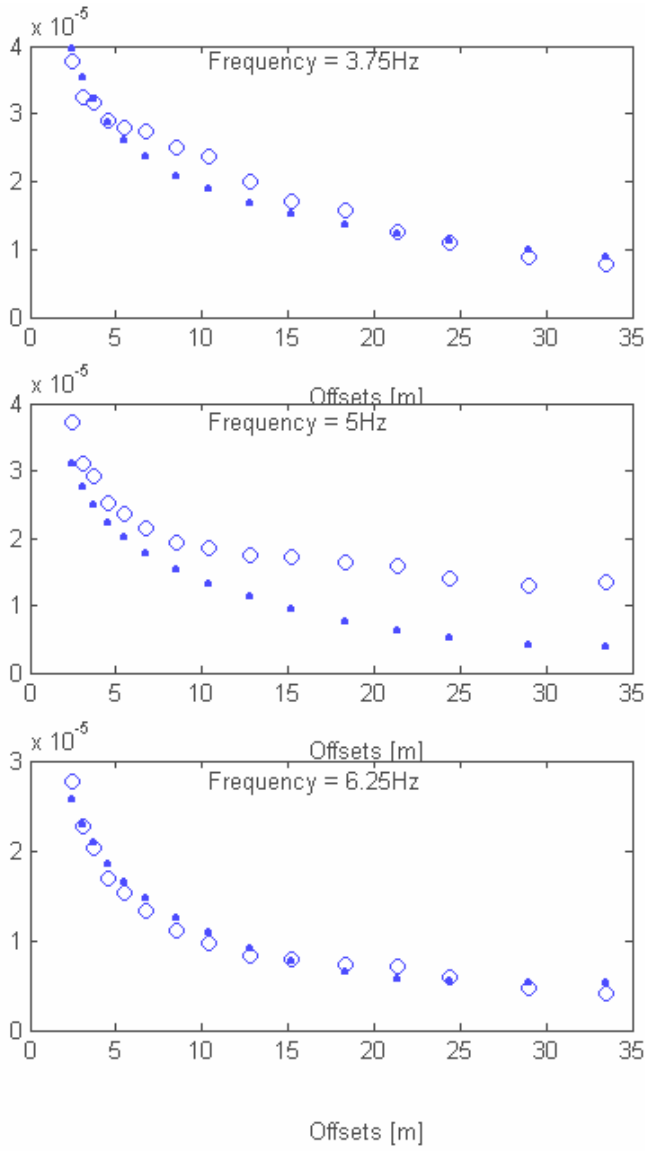


Figure 8. Uncoupled Rayleigh waves method at Mud B site: comparison between experimental (circles) and theoretical (dots) displacement transfer function magnitude at different frequencies for evaluating the experimental attenuation curve.

Table 1. Shear wave velocity and tangent modulus profiles at Mud Island B site by Uncoupled Rayleigh waves method.

Layer	ρ (Kg/m ³)	h (m)	ν Pois- son	Vs (m/s)	Gs (MPa)
1	1800	1.5		195	68
2	1800	1.5	0.2	180	58
3	1800	2.5	0.2	170	52
4	1800	2.5	0.2	170	52
5	1800	5	0.48	165	49
6	1800	6	0.48	190	64
7	1800	7	0.48	280	141
8	1800	10.0	0.48	225	91
Half-space	1800	∞	0.48	665	796

Table 2. Shear damping ratio profiles by means of Rayleigh waves: pure Coupled method, pure Uncoupled method and Hybrid method.

Layer	h (m)	Ds (%)		
		Coupled	Hybrid	Uncoupled
1	1.5	3	3.4	1.5
2	1.5	2.2	3	1.3
3	2.5	1.4	2.5	1.4
4	2.5	2.8	3.8	1.8
5	5	3.3	3.8	3.3
6	6	3.8	3.8	3.5
7	7	3.9	3.8	3.5
8	10.0	4	3.8	3.5
Half-space	∞	4	3.8	3.5

5 CONCLUSIONS

In this work the aim is to illustrate the potentialities of Rayleigh waves propagation method as an in situ technique for site characterization within the range of very small deformations ($\gamma_{cyclic}=5 \cdot 10^{-6} \div 5 \cdot 10^{-5}$). In particular the coupled and the uncoupled Rayleigh waves procedures have provided shear wave velocity and shear damping ratio profiles that are in good agreement with reference to a testing site. Although the coupled procedure is mathematically more rigorous than the uncoupled procedure, the results seem to confirm that at very small deformations the shear tangent modulus and shear damping ratio profiles can be determined independently. In view of engineering applications in the field of dynamic soil-structure interaction, from the results at Mud Island site B and at other sites it has been observed that the attenuation curve for Rayleigh waves generally increases from 0 (1/m) to 0.15 (1/m) in the frequency range (0÷100)Hz and the shear damping ratio varies from 0% to 5% depending on soil nature and conditions as suggested in the literature (Seed H.B. et al. 1984).

6 ACKNOWLEDGMENTS

I am grateful to Prof. J.G.Rix, who kindly provided the experimental data of the Mud Island site B and for his precious teaching during my permanence at Georgia Institute of Technology, Atlanta, GA. I also thank my supervisor Prof. R. Lancellotta of the Technical University of Turin (Politecnico) for his guidance during my PhD research program and Dr. C. Lai, who has spent much of his time discussing with me on the issues contained in the paper.

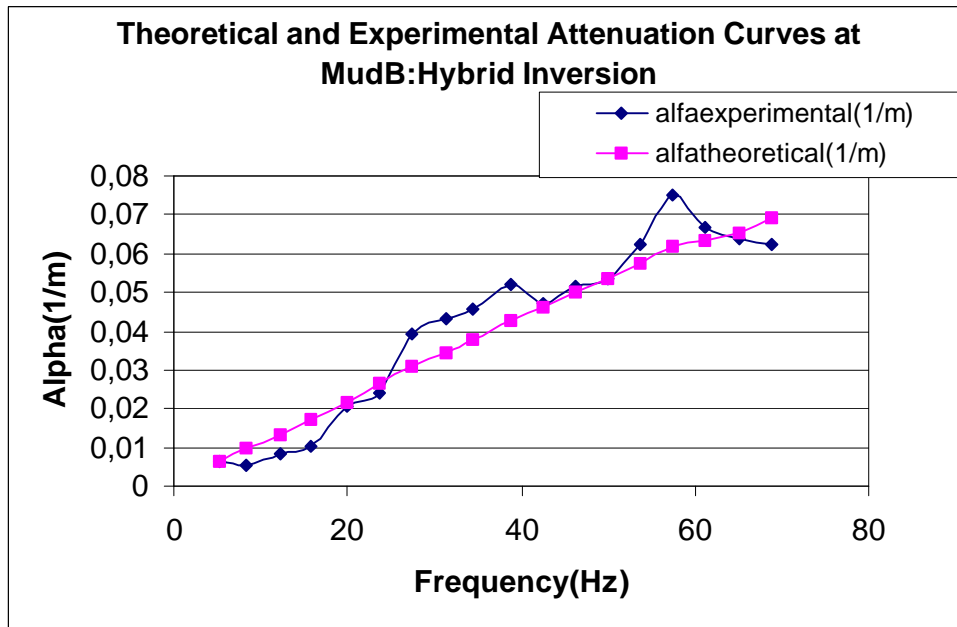


Figure 9. Hybrid Rayleigh waves method at Mud B site: misfit between experimental (diamonds) and theoretical (squares) attenuation curves.

7 REFERENCES

- Achenbach, J.D. 1999. Wave Propagation in Elastic Solids. North-Holland, Amsterdam, Netherlands.
- Aki K. & Richards P.G. 1980. Quantitative Seismology, Theory and Methods, Vol. 1-2 W.H. Freeman & Co., N. York.
- Brillouin, L. & Sommerfeld 1960. Group Velocity
- Christensen, R.M. 1971. Theory of viscoelasticity - an introduction", Ed. Academic Press
- Foti, S. 2000. Multi-Station Methods for Geotechnical Characterization Using Surface Waves. Ph.D Dissertation, Politecnico di Torino (Italy)
- Goldstein, H 1950. Classic Mechanics, Addison Wesley, Reading, Massachussets.
- Haskell, N.H. 1953. The Dispersion of Surface Waves in Multilayered Media, Bulletin of the Seismological Society of America, Vol. 43, pp. 17-34.
- Hebeler, G.L. 2001. Site characterization in Shelby County, Tennessee using advanced surface wave methods. Master's thesis. Georgia Institute of Technology.
- Kausel and Roesset 1981. Stiffness matrices for layered soils, Bulletin of the Seismological Society of America, Vol 71(6), pp. 1743-1761.
- Lai C.G. 1998. Simultaneous inversion of Rayleigh phase velocity and attenuation for near-surface site characterization, PhD Diss., Georgia Inst. of Techn., Atlanta (Georgia, USA)
- Lai G., Rix G., Foti S., Roma V. 2002. Simultaneous Measurement and Inversion of Surface Wave Dispersion and Attenuation Curves, Journal of SDEE 22
- Lancellotta R. 1995. Geotechnical Engineering, A.A.Balkema
- Lighthill, M.J. 1964. Group Velocity, J. Inst. Maths Applics, 1, 1-28
- Mancuso C. 1992. Misura in sito delle proprietà dei terreni mediante prove dinamiche, Tesi di Dottorato (PhD Diss.), Un. Federico II, Napoli (in Italian)
- Mayne, P. 2000. Results of Seismic Piezocone Penetration Tests Performed in Memphis, Tennessee. GTRC Project Nos. E-20-F47/F34 Submitted to USGS/MAE Hazard Mapping Program Central Region By Georgia Tech Research Corporation, Civil & Env. Eng., Atlanta, GA
- Rix G.J. 1988. Experimental study of factors affecting the Spectral-Analysis-of-Surface-Waves method, PhD Diss., Un. of Texas at Austin
- Rix G., Hebeler G., Lai G., Orozco C., Roma V. 2001. Recent Advances in surface Wave Methods for Geotechnical Site Characterization, XV International Conference on Soil Mechanics and Geotechnical Engineering, Istanbul 27-31 Agosto 2001
- Rix G.J., Lai C.G., Wesley Spang A.W. Jr 1999. In situ measurement of damping ratio using surface waves, J. Geotech.and geoenviron. Eng., ASCE
- Roma V. 2001. Soil Properties and Site Characterization by means of Rayleigh Waves. Ph.D Dissertation, Politecnico di Torino (Italy)
- Roma V. 2002. Automated Inversion of Rayleigh Geometrical Dispersion Relation for Geotechnical Soil Identification, 3rd WCSC (World Conference on Structural Control), Como
- Roma V., Hebeler G., Rix G.J., Lai C.G. 2002. Geotechnical Soil Characterisation using Fundamental and Higher Rayleigh Modes Propagation in Layered Media, 12th ECEE London
- Seed H.B., Wong R.T., Idriss I.M., Tokimatsu K. 1984. Moduli and Damping Factors for Dynamic Analysis for Cohesionless Soils, Un. Of California, Berkley, EERC, Report No. EERC 84-14
- Spang, A.W. 1995. In Situ Measurements of Damping Ratio Using Surface Waves, Master's Thesis, Georgia Institute of Technology, Atlanta, GA
- Stokoe II & Santamarina 2000. Seismic-Wave-Based Testing in Geotechnical Engineering, Melbourne
- Thomson, W.T. 1950. Transmission of Elastic Waves Through a Stratified Solid, Journal of Applied Physics, Vol. 21, pp. 89-93.
- Tokimatsu K. 1995. Geotechnical site characterisation using surface waves", Proc. 1st Int. Conf. on Earth. Geotechn. Eng., IS-Tokio, pp. 36
- Tolstoy 1973. Wave propagation, McGraw-Hill, New York
- Vucetic M. 1994. Cyclic threshold shear strains in soils, J. Geotechnical Eng., vol. 120 (12), ASCE, pp. 2208-2228
- Whitham, G.B. 1974. Linear and Non Linear Waves, J. Wiley & sons, New York
- Zywicki D. & Rix G.J. 1999. Frequency-wavenumber analysis of passive surface waves, Proc. Symp. on the Appl. of Geophysics to Environm. and Eng. Problems, Oakland, pp. 75-84